Molecular Dynamics of Surfactant Protein C: From Single Molecule to Heptameric Aggregates

Eunice Ramírez,* Alberto Santana,* Anthony Cruz,* Inés Plasencia,† and Gustavo E. López*
*Department of Chemistry, University of Puerto Rico, Mayagüez, Puerto Rico 00681; and †MEMPHYS, Center for Biomembrane Physics, Department of Biochemistry and Molecular Biology, University of Southern Denmark, DK-5230 Odense M, Denmark

ABSTRACT Surfactant protein C (SP-C) is a membrane-associated protein essential for normal respiration. It has been found that the α-helix form of SP-C can undergo, under certain conditions, a transformation from an α-helix to a β-strand conformation that closely resembles amyloid fibrils, which are possible contributors to the pathogenesis of pulmonary alveolar proteinosis. Molecular dynamics simulations using the NAMD2 package were performed for systems containing from one to seven SP-C molecules to study their behavior in water. The results of our simulations show that unfolding of the protein occurs at the amino terminal, and despite this unfolding, no transition from α-helix to β-strand was observed.

INTRODUCTION

Pulmonary surfactants are essential for normal respiration and lung host defense because they reduce the surface tension in the air-alveolar interface during the breathing process (1). These substances consist of ~79% phospholipids, 8% proteins, 5% neutral lipids, and 8% cholesterol (2). Two of the proteins contained in this mixture complex are membrane associated: surfactant protein B (SP-B) and surfactant protein C (SP-C). These are hydrophobic proteins and are known to enhance the adsorption and dynamic film behavior of phospholipids (3). SP-C has been found to have several functions: i), catalyze the formation of surface-associated micrometer-sized three-dimensional structures at the air-alveolar interface (4,5), ii), assist in the transfer of lipids from the monolayer to form stacked multi-layer structures (6), iii), act as a surfactant protection against inactivation by serum (7,8), and iv), possibly participate in the immune defense (9–12). It has also been proposed that SP-C might regulate the changes in applied lateral pressure in lipid bilayers (13). The role of SP-C in the respiration processes and its function are very similar to that of SP-B, and although it has been widely studied, the molecular level mechanism of action is not fully defined or understood. The properties of SP-C are of particular interest because of their clinical applications.

The SP-C molecule is highly hydrophobic and consists of 35 amino acid residues, which adopt mainly a helical secondary structure conformation. The α-helix includes residues from 9 through 34; the remaining residues (1–9) are not assigned to any specific secondary structural conformation. However, studies with synthetic peptides of this segment demonstrate that the N-terminal segment shows β-turn structure (14). The length and diameter of the helix are ~39 Å and 12 Å, respectively. Native SP-C also contains two fatty acyl chains in the Cys^5 and Cys^6 residues that are thought to stabilize the protein when present in lipid monolayers and bilayers. The helical nature of fully acylated SP-C at the air-water interface has been confirmed by infrared studies. However, some suggest that SP-C helical structure is not the only structure adopted by this molecule (6,15).

It has been shown that under certain solvent and temperature conditions, SP-C is transformed from monomeric α-helix to a polymeric β aggregate which resembles amyloid fibrils (6,16,17). These aggregates have been reported as part of amyloid fibril present during pulmonary alveolar proteinosis (PAP). The deacylation of SP-C has shown an increase in the rate of peptide aggregation and fibril formation because helix destabilization promotes the β aggregation (18). Some studies demonstrate that the amino acid composition of the protein is essential to fibril formation (19) as stated for SP-C (15), although other studies suggest that amyloid fibril formation is a property of the protein backbone (19,20). The SP-C helix is composed primarily of valines, which is unusual since valines are underrepresented in helical conformation and overrepresented in β-strands (15). Because of this, once the helical structure is lost a refold will rarely be observed. However, studies have shown that the β-branched amino acids Val and Ile rank among the best helix promoters in a membrane environment (21). Some pH-dependent experiments have shown that deacylated SP-C adopts an α-helical conformation at low pH, similar to the acylated protein, but an increase in pH has revealed the α-helix to β-strand conformational change (6). The helical structure usually observed in the deacylated SP-C is recovered by lowering the pH. Previous studies indicate that residues 16–20 are essential for α/β intermolecular contacts and fibril formation (15,22), and destabilization of the helix covering residues 17–24 is needed to observe the α-helical to β-sheet transition and later fibril formation (15,23). Specific pathways and causes of SP-C fibril formation are not yet proposed. The behavior of SP-C in environments similar to

Submitted August 25, 2005, and accepted for publication December 28, 2005.
Address reprint requests to Gustavo E. López, Dept. of Chemistry, University of Puerto Rico, PO Box 9019, Mayagüez, PR 00681. Tel.: 787-265-5458; E-mail: eramirez@uprm.edu.

0006-3495/06/04/2698/08 $2.00
doi: 10.1529/biophysj.105.073270

that present in the lung, where water is the main ''solvent'', has not yet been studied either (to our knowledge). Molecular dynamics simulations using the GROMACS 2.0 package have been performed to determine the relative structural stability of SP-C in water and methanol (21). It was found that the α-helix from Asn^{9} to Val^{28} was stable up to a period of 5 ns. On the other hand, the segment comprised of residues Val^{28}–Leu^{32} unfolded in methanol and retained the α-helix structure in water.

In this study, molecular dynamics simulations were performed to determine the relative structural stability of SP-C in water to obtain some insight about the processes suffered by the protein in conditions such as PAP. Specifically, constant temperature, pressure, and number of molecules (NPT) simulations were performed for a system composed of $(SP\text{-}C)_x$ ($x = 1, 2, 3, 6, 7$) molecule(s) solvated in water. Structural changes as a function of time and initial conditions were obtained and related to previous studies.

METHODS

As stated, molecular simulations were performed for depalmitoilated SP-C molecules in water. The system's modeled consisted of one, two, three, six, and seven SP-C molecules with ~8,000 water molecules per SP-C. The protein structure and Cartesian coordinates were downloaded from the Protein Data Bank (PDB code: 1SPF) (24). All simulations were performed using the nonequilibrium Atomic Molecular Dynamics 2 (NAMD2) simulation package version 2.5 (25). The Charmm27 force field (26) was used to model the intramolecular and intermolecular interactions found in SP-C and between SP-C and water molecules. The TIP3P model was used in the description of the water molecules. The SP-C molecules were placed in a rectangular box with periodic boundary conditions in all directions. Long-range electrostatic interactions were calculated using the particle mesh Ewald (PME) method (27) with a 12 Å cutoff for electrostatic and van der Waals interactions. All h-bonds' (h-bond) lengths were held constant with the SHAKE-RATTLE-ROLL algorithm. The simulations were carried out at an NPT ensemble with a temperature of 310 K, which resembles normal body temperature. A Langevin thermostat with a coupling constant of 5 ps^{-1} was used to fix the temperature. The pressure was isotropically maintained by coupling it to a Langevin barostat at 1 atm with an oscillation time of 100 fs and a damping time of 50 fs. The lengths of the simulations were determined by the proper convergence of the properties computed. Specifically, for one, six, and seven SP-C molecules the simulations ran for a period of 10 ns, whereas the remaining systems were run for ~5 ns. The time step for all simulations was set to 2 fs. Trajectory analysis and molecular graphics images were generated using the Visual Molecular Dynamics (VMD) software (28). Root mean-square deviation analyses (RMSD) were performed to evaluate systems mobility and proper convergence, i.e., when no variation in the RMSD was observed, the simulation was terminated. The time evolution of the radius of gyration (Rgyr), end-to-end distance, solvent accessibility surface area (SASA), and h-bond interactions were monitored during the simulation. Ramachandran plots and timeline diagrams were generated to determine how the secondary structure of the protein changed over time.

Fig. 1 shows the initial arrangement of some of the SP-C systems used in this work. The systems were generated using the original helical structure of the molecule obtained from the PDB file. For the system with one SP-C, the molecule was placed in a rectangular simulation box and solvated with water. The solvation was performed using VMD, with water molecules filling the gaps between chains in systems with more than one SP-C. The size of the box was specified and chosen so the SP-C would not interact with its images. For the multi-protein systems, each protein was placed at a distance of 10 Å from an axis that goes through the center of the α-helix. Hence, the closest atoms (which are hydrogens on different chains) are at a distance of ~1 Å, which did not cause any undesired perturbation on the system. Fig. 1 *A* shows the geometrical arrangement of two SP-C molecules where the chains are in a parallel orientation to one another. The amino terminals were pointing in opposite directions. All other systems modeled in this work had their amino terminals pointing in the same direction. Two different geometries were used for the system of three SP-C molecules: a triangular arrangement (TA) shown in Fig. 1 *B* and a linear arrangement (LA) not shown. Fig. 1 *C* shows how the six SP-C molecules were arranged in a hexagonal pattern. The system consisting of seven SP-C molecules was constructed by placing an SP-C molecule in the center of the hexagonal arrangement.

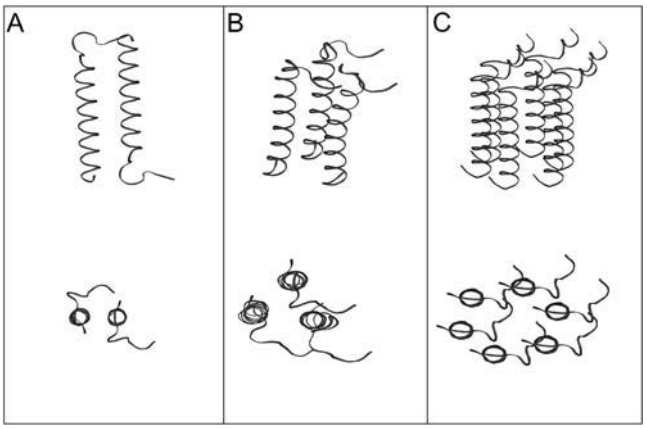

FIGURE 1 Molecular arrangements for two (*A*), three (*B*), and six (*C*) SP-C molecules. Each panel shows both a lateral and top view of the systems.

After preparing the initial structures, a minimization procedure was performed on all systems for 20 ps. In the case of the multi-protein systems, the separation between the chains increased by several angstroms and hence more water was accommodated between the chains.

It is important to mention that various procedures and geometrical patterns were used to generate the initial structures. However, this procedure has proven to be the most efficient and gave better convergence of the calculated properties. Moreover, we are interested in observing the time evolution of the various systems starting from the native structure of the single protein in a timescale dictated by the computational resources available.

RESULTS

To analyze the behavior of each SP-C molecule during the simulations, the time evolution of the secondary structure, RMSD, Rgyr, and SASA were calculated. Fig. 2 shows the RMSD values calculated for each SP-C system during the simulations. For most of the systems, the RMSD does not fluctuate more than 3.0 Å from its average value during the last 2 ns of the simulation. Hence, as explained in previous studies (29), if the simulation reached an RMSD that oscillates around a constant value, it can be assumed that the system has converged to a stable or a metastable structure. Our results for the Rgyr and end-to-end distance analysis provide similar information; therefore, the unfolding of the systems will be discussed primarily based on the secondary structure evolution and the end-to-end distance analysis. Table 1 shows a time average (over all chains) of the RMSD,

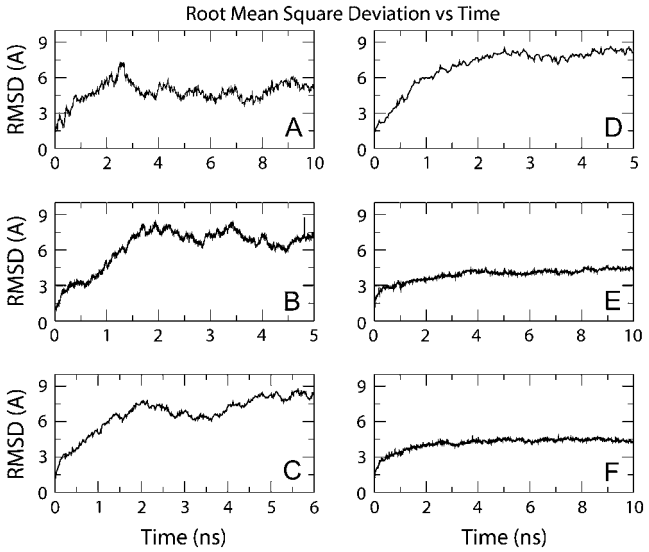

FIGURE 2 Graphical representation of the RMSD analysis over time for the SP-C systems (*A*) single molecule, (*B*) two molecules, (*C*) three molecules (LA), (*D*) three molecules (TA), (*E*) six molecules, and (*F*) seven molecules.

end-to-end distance, Rgyr, and SASA quantities over the last 2 ns of the simulations. The secondary structure assigned to the chains represents the conformation that the protein predominantly adopted during the selected time range, and this information is summarized in Table 2. The original conformation of SP-C is also included for comparison purposes. At the beginning of the simulation each SP-C chain has 26 amino acid residues forming the α-helix domain, which represents 74.1% of the protein residues. The remaining residues belong to a random coil or β-turn structure representing the 25.7% of the amino acids.

The single SP-C molecule/water system reached a stable RMSD at ~4 ns (Fig. 2 *A*). At the end of the simulation, SP-C did not exhibit significant changes in terms of the number of amino acids forming the secondary structure. Fig. 3 shows the secondary structure evolution in a timeline board, where the colors pink, red, white, and blue represent the α-helix, π-helix, random coil, and β-turn domains, respectively. It is observed that only two residues that were initially part of the helix domain unfolded and became part of the β-turn domain. Additionally, the α-helix changed to a π-helix, decreasing the length of the helix from 35.7 to 28.1 Å. Changes in the helix were observed starting from the carboxy terminal to a few amino acids away from the amino terminal. After 10 ns of simulation time, 19 residues (18–31) comprised the π-helix and the remaining five amino acids (8–12) remained in an α-helix structure domain. The preservation of the SP-C helical structure, with water as the solvent, has been discussed elsewhere (21), although the helical transformation ($\alpha \rightarrow \pi$) has not been mentioned. Preservation of the helix could be understood in terms of a cooperative packing structure formed by the hydrophobic β-branched side chains. This packing effect is also supported by the reduction observed in the SASA values for this system, which decreased by 250 Å^2 from its initial value. The end-to-end distance analysis shows that the molecule length was reduced during the simulation, as demonstrated by the secondary structure analysis.

In general, in the two SP-C molecules simulation, no significant changes were observed in the secondary structure contents of the system. The secondary structure of chain 2 closely resembles that of the original SP-C. Chain 1 showed, at several points during the simulation, a tendency to form a π-helix conformation with residues 23–26. This chain also exhibited a weakening of the helix packing interaction in portions of the α-helix (Ile^{27}, Val^{28}, Gly^{29}). These amino acid residues' backbone angles were assigned to a β-turn domain. Although this chain suffered changes in its helix domain related to unfolding, the Rgyr, SASA, and end-to-end

TABLE 1 Average values of RMSD, Rgyr, system SASA, and end-to-end distance (*D*)

SP-C System	RMSD (Å)	Rgyr (Å)	*D* (Å)	SASA (Å^2)
1	5.3 ± 0.4	13.8 ± 0.5	45 ± 3	3513 ± 60
2	7.0 ± 0.5	15.8 ± 0.5	46 ± 3	3044 ± 11
3 (LA)	8.0 ± 0.4	18.1 ± 0.2	46 ± 4	3809 ± 198
3 (TA)	4.4 ± 0.1	15.7 ± 0.2	45 ± 2	2774 ± 43
6	4.4 ± 0.1	19.5 ± 0.1	50 ± 3	2628 ± 48
7	4.4 ± 0.1	19.6 ± 0.1	51 ± 2	2598 ± 74

TABLE 2 Amino acids secondary structure domain assignment

No. SP-C molecules	Chain	Random coil/β-turn domain (%)	Helical domain (%)
1	Original	25.7	74.3
1	1	31.4	68.6
2	1	34.3	65.7
	2	25.7	74.3
	1	40.0	60.0
3 (LA)	2	45.7	54.3
	3	34.3	65.7
	1	31.4	68.6
3 (TA)	2	28.5	71.4
	3	25.7	74.3
	1	34.3	65.7
	2	31.5	68.5
6	3	22.9	77.1
	4	34.3	65.7
	5	31.4	68.6
	6	42.9	57.1
	1	28.6	71.4
	2	25.7	74.3
	3	28.6	71.4
7	4	34.3	65.7
	5	31.4	68.6
	6	34.3	65.7
	7	40.0	60.0

Chains average values calculated from the domains represented in the secondary structure evolution board.

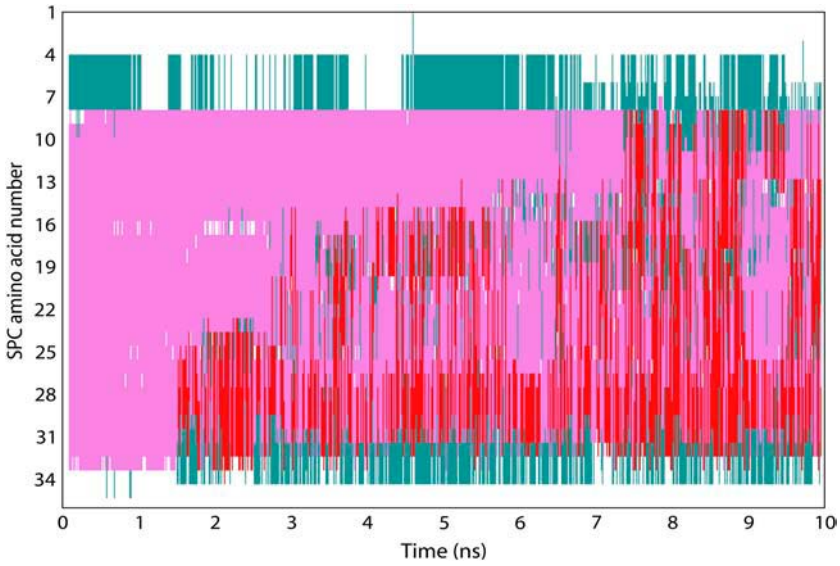

FIGURE 3 Single SP-C secondary structure evolution board. Coloring code: pink, α-helix; red, π-helix; white, random coil; and blue, β-turn.

distance values obtained were lower than those obtained for chain 2 due to a bending in this chain close to the carboxy terminal. It has been proposed that the helix unfolding occurs by solvent insertion, which leads to a weakening of the helix backbone interactions (21); however, chain 1 did not show an increase in the number of h-bonds with the solvent.

Molecular dynamics simulations of two different arrangements of the three SP-C molecules were carried out, as previously described. Fig. 4 presents snapshots of this system at different times during the simulation. Both simulations showed an overall constant RMSD value after 3 ns (Fig. 2, *C–D*) with a system average RMSD of 8.0 Å for both the LA and TA arrangements. This suggests a decrease in the mobility of the chains in a packed arrangement. In the LA all the chains showed a decrease in the number of amino acids comprising the helical domain. Chain 2 exhibited the highest degree of unfolding where only 19 amino acid residues formed the helix at the end of the simulation. Some of the unfolding of chain 1 and 2 occurred in the amino acids 14–17 and 18–20, respectively. These regions have been identified as essential for helical destabilization and/or α/β intermolecular contacts that might lead to fibril formation (15,22,23). In addition to the unfolding in some residues close to the amino terminal, chain 3 suffered a helix-type transition in which amino acids Val^{28}–Leu^{32} comprised a π-helix. The Rgyr analysis showed that two of the chains increased their initial length after 6 ns, whereas the other gets shorter. Although the chains in the TA preserved the helical structure, chain 2 exhibited a change similar to that observed with the single SP-C molecule, that is the helix type changed from α-helix to π-helix. After 4 ns, the α-helix was formed by 6 of the 25 residues assigned to the helical domain.

In the system with six SP-C molecules, the chains were placed in a hexagonal arrangement as shown in Fig. 1 *C*. Fig. 5 shows each SP-C chain at different stages of the simulation. It clearly shows how chains 4 and 5 undergo a translational/rotational motion until they get aligned with the other chains, forming a system similar to the LA. This displacement maximizes the SP-C···SP-C interactions, thus, decreasing the number of available sites to which solvent

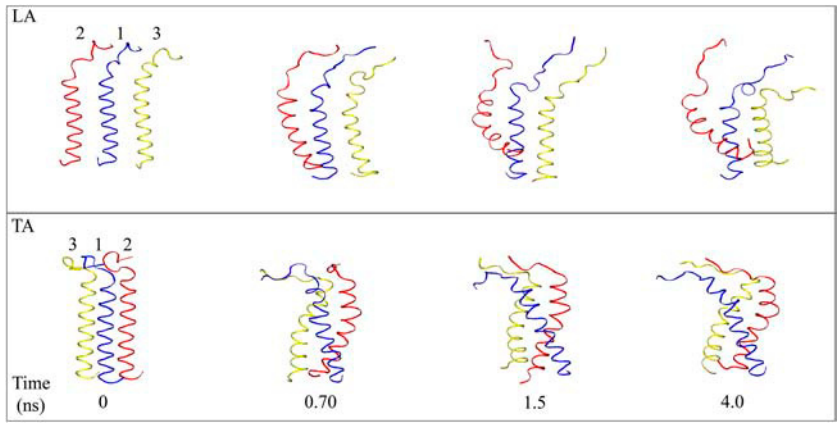

FIGURE 4 Snapshots of the $(SP\text{-}C)_3$ systems at different times.

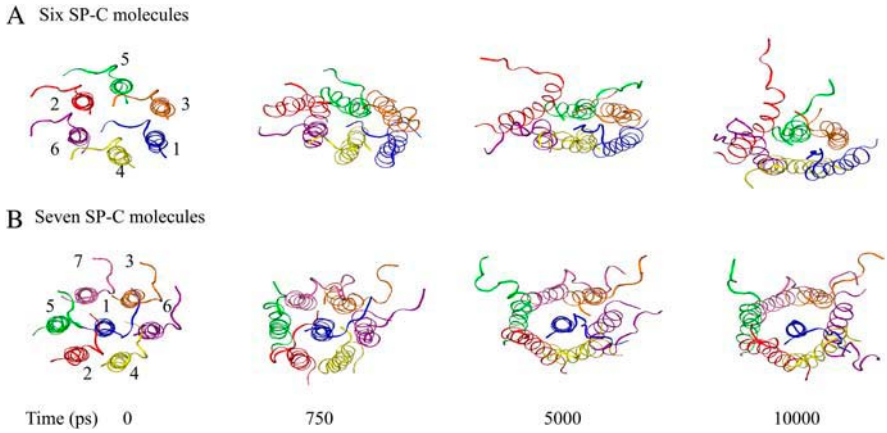

FIGURE 5 Snapshots of the $(SP\text{-}C)_6$ and $(SP\text{-}C)_7$ systems at different times.

molecules have access. At the same time, the chains adopted a tilted orientation that could stabilize the system. This orientation is similar to what is observed in proteins containing α-helical bundles. Fig. 6 shows the chains' secondary structure evolution in a timeline board. Chains 2 and 6 exhibited a different secondary structure behavior compared to the others. Chain 6 showed a decrease in the number of amino acids forming the α-helix structure, which after 10 ns contained 19 residues compared to the original structure, which has 26. The change observed in chain 2 can be identified as a helix type transformation from $\alpha \rightarrow \pi$-helix. After 10 ns the α-helix contained 18 of the 24 residues assigned to a helical domain. Conformational changes from a β-turn to a random coil domain were also observed in some of the SP-C chains on this system. The end-to-end distance values for the individual chains fluctuated between 36 and 60 Å, with chain 2 being the one that gave the lowest value. This fact directly relates to the helical change suffered by this chain. In general, the average end-to-end distance results (50.5 Å) suggest that the lengths of the chains are increasing compared to the previously discussed results, which showed average values fluctuating from 45.5–45.9 Å.

An SP-C molecule was placed at the center of the six molecules SP-C arrangement to perform the seven molecules simulations. The RMSD shows (Fig. 2 *F*) that the system chains' mobility decreased after 5 ns, with values per chain ranging from 5.0 to 7.0 Å. Our results showed a conservation of the original SP-C arrangement, thus suggesting a stabilization of the system due to the inserted SP-C molecule. The secondary structure analysis showed, as observed with the six SP-C simulation, that two chains behave differently. Chain 5 contained a β-turn domain (Leu^{13}–Leu^{14}) between a π-helix (Val^{8}–Arg^{12}) close to the amino terminal and an α-helical domain. At a given point in the simulation, the β-turn domain was composed of the sequence Leu^{13}–Val^{18}. However, as the π-helix was formed this range decreased to just two amino acids (Leu^{13} and Leu^{14}). Chain 7 unfolded to a higher degree than the other chains. The end-to-end distance

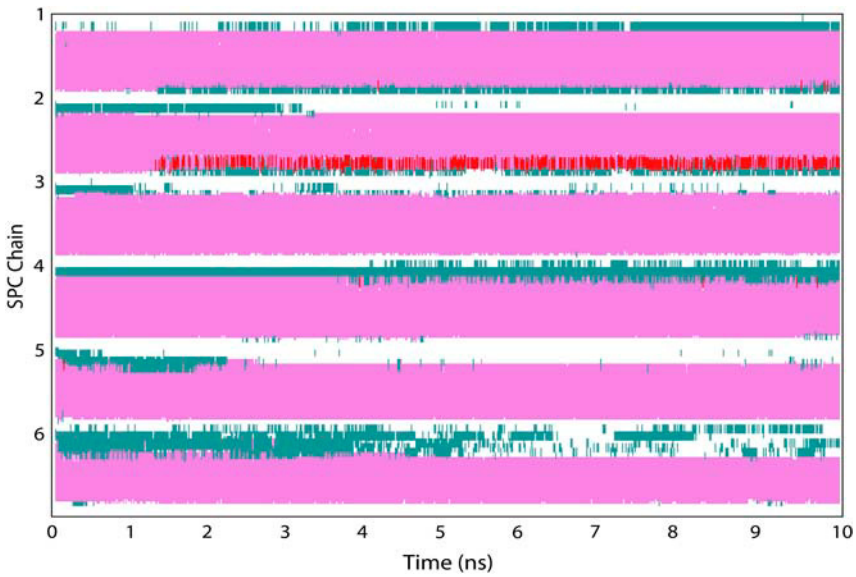

FIGURE 6 Secondary structure evolution board for the $(SP\text{-}C)_6$ system.

analysis showed a system average value of 50.6 Å. The RMSD values obtained seem not to be directly related with the Rgyr; i.e., chain 5, which had a high mobility and showed significant changes in its backbone helix interaction, is the chain with the lower end-to-end distance and Rgyr.

DISCUSSION

Previous studies have shown that the α-helix to β-sheet transformation is required for the amyloidal fibrils formation. In vitro, SP-C fibrils are formed in polar organic solvent mixtures which reduce hydration of the protein surface and enhance intermolecular h-bonds, leading to protein aggregation (19). Previous molecular dynamics simulations demonstrate that the SP-C helix unfolds to a higher degree in methanol compared to water (21), where unfolding occurred at the carboxy terminal. As a general result, unfolding of the protein in our simulations occurred at the amino terminal, although some unfolding was observed within the original helical domain. Regardless of the degree of helix unfolding, no α-helix to β-strand transformation was observed with the environmental conditions and timescales of our simulations; therefore, no amyloidal fibrils were formed in this timescale.

The secondary structure pattern observed is independent of the system size: i), one chain remains almost identical to the initial SP-C molecule; ii), one chain exhibited some degree of $\alpha \rightarrow \pi$-helix transformation, as observed with one SP-C; and iii), one chain unfolds to a higher degree compared to the others. Based on the results observed with the single molecule simulation, as the molecule is exposed to a destabilizing environment the helical structure slightly changed to decrease the protein-solvent interactions. However, as more SP-C molecules were added the SP-C···SP-C interactions seemed to decrease the solvent effect; therefore, a higher degree of unfolding was observed in the systems. The SP-C···SP-C interactions were analyzed based on the conztacts observed at some stages during the simulation. A chain-to-chain interaction was assigned based on the backbone-to-backbone distances, i.e., the chains were considered to be interacting whenever the backbone-to-backbone distance was $\leq$8 Å (30). The regions in which these interactions occurred varied from chains and the system considered. In 50% of the cases, the amino acids involved in the interaction were from residues 16–24, which are known to be essential intermolecular contacts to induce helix destabilization and fibril formation (15,22,23). The amino acid residues comprised in this region are valines, except for the leucine 22. Some chains in the six and seven molecules systems showed a high degree of interaction with the residues comprised in the amino terminal, but rarely through the residues at the carboxy terminal. The motifs observed in the chain-to-chain interactions in the six and seven molecules systems resemble the knobs-into-holes packing observed in membrane and soluble α-bundle proteins (30). On the other hand, we found an increase in the chain-to-chain h-bond formation between a pair of chains in the systems. Most of the chains that exhibit this increase in h-bond formation also showed a weakening in the helix packing intramolecular interactions. The h-bonds analysis showed that many SP-C chains suffered a reduction in the number of intramolecular h-bonds during the simulation, whether their intermolecular h-bonds change or not. In the LA model system, the calculated SASA values for the total system increased during the simulation, opposed to the TA in which the SASA remained relatively constant; however, no h-bond increase was observed between proteins and solvent. Although the solvent might have some important interactions with the less packed systems (one, two, and LA), we observed no h-bond increase between the protein chains and the solvent during the simulation. The contacts and h-bonds analyses lead us to suggest that the vicinity of SP-C chains induces structural changes primarily due to van der Waals interaction. Systems with six and seven SP-C molecules showed a minimal increase in the SASA, but individually some chains showed an increase in their values. These chains also showed a slight increase in the number of h-bonds with the solvent. In all systems considered, a solvation shell was observed at a distance of ~3.0 Å from the protein boundaries.

A helix-helix interaction was observed in all the multi-SP-C systems, with the SP-C chains tilted with respect to one another. This behavior could place the system in an energetically accessible state. Fig. 7 shows a plot of helix tilt angle over time for the six and seven molecules systems. The tilt angle was determined with respect to each SP-C chain in the initial conformation of the system. If the SP-C helical domain showed any kind of interruption, the portion with the longer helical domain was used to determine the tilt angle. After 10 ns the average SP-C tilt angle for the six and seven molecules systems were 21.8° and 25.1°, respectively. The observed average values of the tilt angles are similar to the

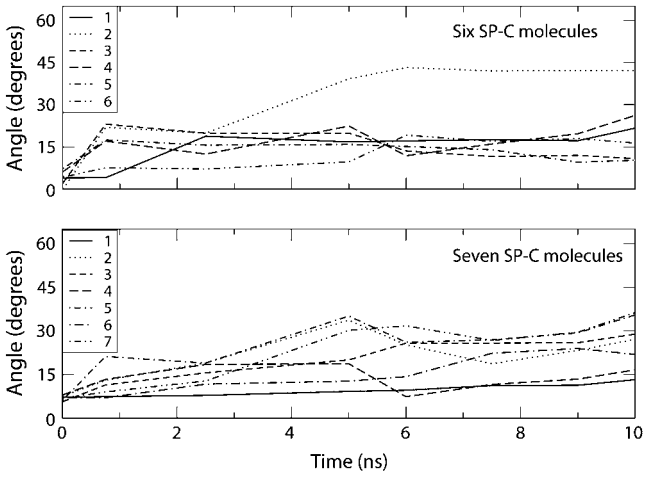

FIGURE 7 Graphical representation of the SP-C chains tilt angle evolution in the six and seven molecules systems. Each graphic represents the tilt angle of each SP-C.

one found in membrane proteins which has been reported to be ~22° (31). The SP-C chain 2 in the six molecules simulation reaches an angle 20° higher than the average values, which could be related to the exhibited transition from α-helix to π-helix.

SUMMARY

In this work, we presented molecular dynamics simulations of several SP-C systems solvated by water. The results were analyzed by considering different properties: the secondary structure evolution to determine the degree of unfolding of the protein, RMSD, Rgyr, h-bonds, end-to-end distance, and SASA were calculated to evaluate system general behavior. The results of the single SP-C molecule simulation are in agreement with previous works where the SP-C molecule maintained its helical domain in water (21). Although definitely not in perfect agreement with experiments, our results for the multi-chains SP-C systems have shown interesting trends. No amyloid fibril formation was observed in the systems with the modeled environmental conditions in the time range considered. However, important secondary structural changes were observed and these are believed to destabilize the protein and weaken the intramolecule interactions which could lead to fibril formation. It is important to point out the fact that our simulations used water as solvent, contrary to other works (15,21) in which organic solvents were used. This suggests that the solvent could play an important role in the process of amyloid fibril formation. Helix unfolding predominantly occurred at the protein amino terminal. No significant increase in protein-water h-bonds was observed, except for some chains in the six and seven SP-C molecules systems. We found no correlation between the chain-to-chain contacts and the number of h-bonds between these chains. These results suggest that van der Waals interaction might play a major role in the simulated systems. A significant number of the SP-C···SP-C contacts were found in the region composed of residues 16–24, which has been determined to play a major role in SP-C fibril formation (15,22,23). The SASA analysis suggests that solvent effects on the different chains are variable depending of the number of SP-C chains in the system. The large range of values of the helix tilt angle observed in the six and seven molecules systems could be a consequence of the absence of a constraining media, opposed to what is observed with membrane proteins where lipids molecules might inhibit a less varying tilt angle. In membrane environments the adopted helix tilt angle usually is ~22°.

Amyloid fibril formation is a complex process which has been identified to occur via the following steps: local unfolding of the native protein, intermolecule association, structural rearrangement which increases β-sheet content, and cross-β-sheet polymerization (15). Thus the timescales at which these events can be observed are out of our simulation time ranges. However, the results presented in this work give important insight concerning the protein-protein interactions that SP-C molecules exhibit before the unfolding takes place. At present parallel tempering and steered molecular dynamics calculations are being performed to get a better understanding of the behavior of these systems and equilibrium properties. We are also carrying out calculations of SP-C in lipid monolayers and membranes to obtain some insight into the processes in which the protein is involved.

We thank Dr. Jorge L. Ríos-Steiner for constructive comments and discussion on this work.

This work is supported by grants from the National Institutes of Health SCORE (grant No. GM008103-03) and National Institutes of Health COBRE (grant No. P20RR16439-01) programs.

REFERENCES

1. Clements, J. 1970. Pulmonary surfactant. *Am. Rev. Respir. Dis.* 101: 984–990.
2. Daniels, C., and S. Orgeig. 2001. The comparative biology of pulmonary surfactant: past, present and future. *Comp. Biochem. Phys. A.* 129:9–36.
3. Weaver, T. E., and J. Conkright. 2001. Function of surfactant proteins B and C. *Annu. Rev. Physiol.* 63:555–578.
4. Krüger, P., M. Schalke, Z. Wang, R. H. Notter, R. A. Dluhy, and M. Losche. 1999. Effect of hydrophobic surfactant peptides SP-B and SP-C on binary phospholipids monolayer. *Biophys. J.* 77: 903–914.
5. Krüger, P., J. E. Baatz, R. A. Dluhy, and M. Lösche. 2002. Effect of the hydrophobic peptide SP-C on binary phospholipid monolayer. Molecular machinery at the air/water interface. *Biophys. Chem.* 99: 209–228.
6. Dluhy, R. A., S. Shanmukh, J. B. Lepard, P. Krüger, and J. E. Baatz. 2003. Deacylated pulmonary surfactant protein SP-C transforms from alpha-helical to amyloid fibril structure via pH-dependent mechanism: an infrared structural investigation. *Biophys. J.* 85: 2417–2429.
7. Amirkhanian, J. D., R. Bruni, A. J. Waring, and H. W. Taeusch. 1991. Inhibition of mixtures of surfactant lipids and synthetic sequences of surfactant proteins SP-B and SP-C. *Biochim. Biophys. Acta.* 1096: 355–360.
8. Amirkhanian, J. D., R. Bruni, A. J. Waring, C. Navar, and H. W. Taeusch. 1993. Full length synthetic surfactant proteins, SP-B and SP-C, reduced surfactant inactivation by serum. *Biochim. Biophys Acta.* 1168:315–320.
9. Augusto, L. A., M. Synguelakis, Q. Espinassous, M. Lepoivre, J. Johansson, and R. Chaby. 2003. Cellular antiendotoxin activities of lung surfactant protein C in lipid vesicles. *Am. J. Respir. Crit. Care Med.* 168:335–341.
10. Augusto, L. A., M. Synguelakis, J. Johansson, T. Pedron, R. Girard, and R. Chaby. 2003. Interaction of pulmonary surfactant protein C with CD14 and lipopolysaccharide. *Infect. Immun.* 71:61–67.
11. Augusto, L. A., M. Synguelakis, J. Johansson, and R. Chaby. 2002. Structural basis for interactions between lung surfactant protein C and bacterial lipopolysaccharide. *J. Biol. Chem.* 277:23484–23492.
12. Augusto, L. A., K. L. Blay, G. Auger, D. Blanot, and R. Chaby. 2001. Interaction of bacterial lipopolysaccharide with mouse surfactant protein SP-C molecular dynamics 13 C inserted into lipid vesicles. *Am. J. Physiol. Lung Cell. Mol. Physiol.* 281:L776–L785.
13. Baatz, J. E., K. L. Smyth, J. A. Whitsett, C. Baxter, and D. R. Absolom. 1992. Structure and functions of a dimeric form of surfactant protein SP-C: a Fourier transform infrared and surfactometry study. *Chem. Phys. Lipids.* 63:91–104.

14. Plascencia, I., L. Rivas, K. M. Keough, D. Marsh, and J. Perez-Gil. 2004. The N-terminal segment of pulmonary surfactant lipopeptide SP-C has intrinsic propensity to interact with and perturb phospholipid bilayers. *Biochem. J.* 377:183–193.

15. Johansson, J. 2003. Molecular determinants for amyloid fibril formation: lessons from lung surfactant protein C. *Swiss Med. Wkly.* 133: 275–282.

16. Szyperski, T. G., G. Vandenbussche, T. Curstedt, J. M. Ruysschaert, K. Wuthrich, and J. Johansson. 1998. Pulmonary surfactant-associated polypeptide C in a mixed organic solvent transforms from a monomeric α-helical state into insoluble β-sheet aggregates. *Protein Sci.* 7:2533–2540.

17. Gustafsson, M., J. Thyberg, J. Näslund, E. Eliasson, and J. Johansson. 1999. Amyloid fibril formation by pulmonary surfactant protein C. *FEBS Lett.* 464:138–142.

18. Gustafsson, M., W. J. Griffiths, E. Furusjo, and J. Johansson. 2001. The palmitoyl groups of lung surfactant protein C reduce unfolding into a fibrillogenic intermediate. *J. Mol. Biol.* 310:937–950.

19. Ohnishi, S., and K. Takano. 2004. Amyloid fibrils form the viewpoint of protein folding. *Cell. Mol. Life Sci.* 61:511–524.

20. Guijarro, J. I., M. Sunde, J. A. Jones, I. D. Campbell, and C. M. Dobson. 1998. Amyloid fibril formation by SH3 domain. *Proc. Natl. Acad. Sci. USA.* 95:4224–4228.

21. Zangi, R., H. Kovacs, W. F. Gunsteren, J. Johansson, and A. E. Mark. 2001. Free energy barrier estimation of unfolding the α-helical surfactant-associated polypeptide C. *Proteins.* 43:395–402.

22. Tjernberg, L. O., J. Näslund, F. Lindqvist, J. Johansson, A. R. Karlstrom, and J. Thyberg. 1996. Arrest of β-amyloid fibril formation by a pentapeptide ligand. *J. Biol. Chem.* 271:8545–8548.

23. Janek, K., S. Rothemund, K. Gast, M. Beyermann, J. Zipper, H. Fabian, M. Bienert, and E. Krause. 2001. Study of the conformational transition of A β(1–42) using D-amino acid replacement analogues. *Biochemistry.* 40:5457–5463.

24. Johansson, J., T. Szyerski, T. Curstedt, and K. Wuthrich. 1994. The NMR structure of the pulmonary surfactant-associated polypeptide SPC in an apolar solvent contains a valyl-rich alpha-helix. *Biochemistry.* 33:6015–6023.

25. Kalé, L., R. Skeel, M. Bhandarkar, R. Brunner, A. Gursoy, N. Krawetz, J. Phillips, A. Shinozaki, K. Varadarajan, and K. Schulten. 1999. NAMD2: greater scalability for parallel molecular dynamics. *J. Comput. Phys.* 151:283–312.

26. Feller, S. E., D. X. Yin, R. W. Pastor, and J. A. D. Mackerell Jr. 1997. Molecular dynamics simulation of unsaturated lipid bilayers at low hydration: parameterization and comparison with diffraction studies. *Biophys. J.* 73:2269–2279.

27. Essmann, U., L. Perera, M. L. Berkowitz, T. Darden, H. Lee, and L. G. Federsen. 1995. A smooth particle mesh Ewald method. *J. Chem. Phys.* 103:8577–8593.

28. Humphrey, W., A. Dalke, and K. Schulten. 1996. VMD—Visual Molecular Dynamics. *J. Mol. Graph.* 14:33–38.

29. Villa, E., A. Balaeff, and K. Schulten. 2005. Structural dynamics of the lac repressor-DNA complex revealed by a multiscale simulation. *Proc. Natl. Acad. Sci. USA.* 102:6783–6788.

30. Eilers, M., A. B. Patel, W. Liu, and S. O. Smith. 2002. Comparison of helix interactions in membrane and soluble α-bundles proteins. *Biophys. J.* 82:2720–2736.

31. van der Wel, P. C., E. Strandberg, J. A. Killian, and R. E. Koeppe II. 2002. Geometry and intrinsic tilt of a tryptophan-anchored transmembrane α-helix determined by ^{2}H NMR. *Biophys. J.* 83:1479–1488.